FDC Progress Report (September 2006)

Simon Taylor
Ohio University

Daniel S. Carman
Jefferson Lab

David Lawrence
Jefferson Lab

Brian Kross
Jefferson Lab

September 25, 2006

Abstract

This note describes progress toward the design of a full-scale FDC prototype based on resolution studies of the small-scale prototype and construction of mechanical jigs for tensioning the cathode planes. Preliminary results for the nominal field+sense wire plane configuration are presented.

1 Introduction

The Forward Drift Chamber (FDC) system consists of a set of 24 planar drift chambers grouped into four sets of six chambers designed to track forward-going particles in the GlueX detector. Figure 1 shows the position of the FDC packages within the GlueX detector. Each chamber consists of a wire plane flanked on either side by cathode planes divided into strips as illustrated

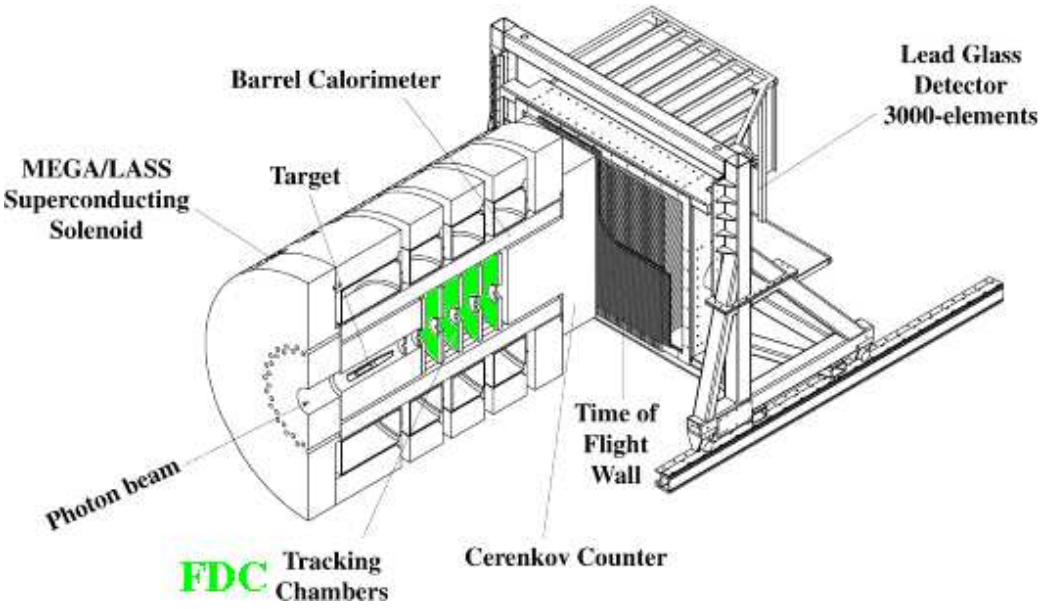

Figure 1: The GlueX detector.

in figure 2. The strips in each view are oriented at 45° with respect to the wires and 90° with respect to the opposing view. The purpose of crossing the strips in this manner is to aid pattern recognition. The wire plane consists of alternating field and sense wires. The nominal design parameters are tabulated in table 1.

The purpose of the field wires is to shape the field to provide better drift time characteristics in the critical region near the edges of a drift cell (5 mm from a given sense wire). Figure 3 shows the results of Garfield calculation for the case where the high voltage on the sense and field wires is +1650 V and -300 V, respectively. Equal numbers of field lines terminate on the cathode planes and the field wires. The field strength near the wires and the surface charge density for this configuration are listed in table 2. Garfield results for other high voltage combinations are described in [1]. Figure 4 illustrates that the long-time edge of the drift time distribution is poorly defined when the field wires are absent but the distribution becomes sharper when the field wires are present, especially when the magnitude of the voltage on the field wires is increased. The effect of changing the field wire high voltage on the position resolution derived from the cathode strip data is described in section 3.

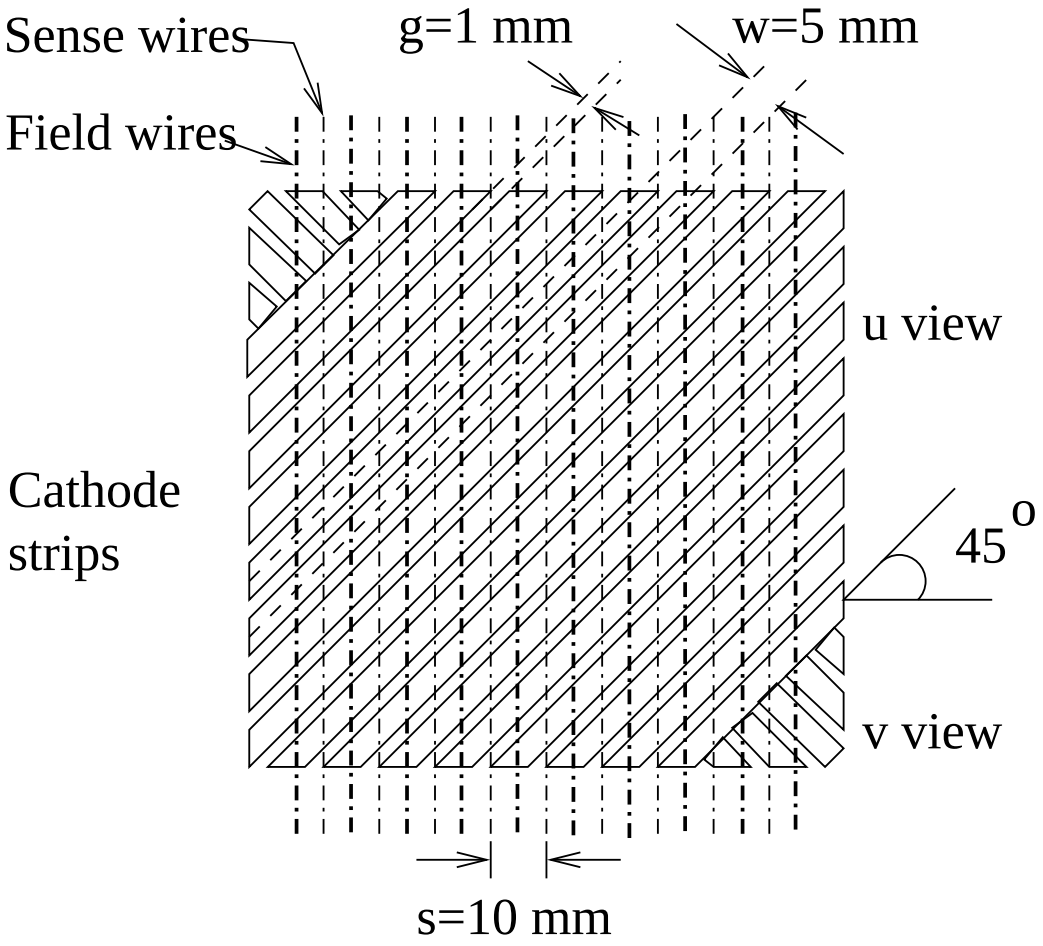

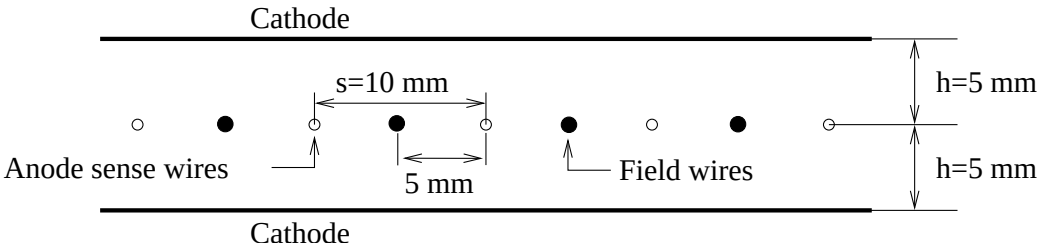

Figure 2: Sketches of the geometry of one FDC chamber.

Parameter	Value
Wire spacing s	10 mm (anode-anode) 5 mm (anode-field)
Anode-cathode distance, d	5.0 mm
Cathode readout pitch, w	5.0 mm
Gap between cathode strips, w_g	1.0 mm
Width of cathode strips	4.0 mm
Capacitance between strips	21 pF/m
Total strip capacitance	56 pF/m + 8 pF
Resistance between strips	$\sim$20 MΩ
Anode wire radius, r_a	0.010 mm
Wire capacitance per unit length, C_0	$\sim$9 pF/m
Gas gain	5×10^5
Operating voltage at nominal gain	1800 V
Electric field at cathode, E_c	$<$1 kV/cm
Electric field on anode wire surface	280 kV/cm
Field-shaping wire radius	0.040 mm
Electric field on field-shaping wire surface	15 kV/cm
Positive ion mobility, μ^+	1.3 cm^2/V/s
Total ion pairs	94/cm
Minimum wire tension	50 gm
Total charge collected	$\sim$15.5 pC
Charge collected in 30 ns (%)	$\sim$20%

Table 1: Nominal FDC Specifications

	Charge	Surface field (kV/cm)	Field at 2r (kV/cm)	Surface pot. (volts)	Pot. at 2r (volts)
Sense wire	263.68	263.68	131.84	1650.0	1467.2
Field wire	-113.49	16.21	8.11	-300.0	-221.3

Table 2: Charge, surface electric field, electric field at twice the wire radius, surface potential, and potential at twice the wire radius for the wire plane with +1650 V on the sense wires and -300 V on the field wires.

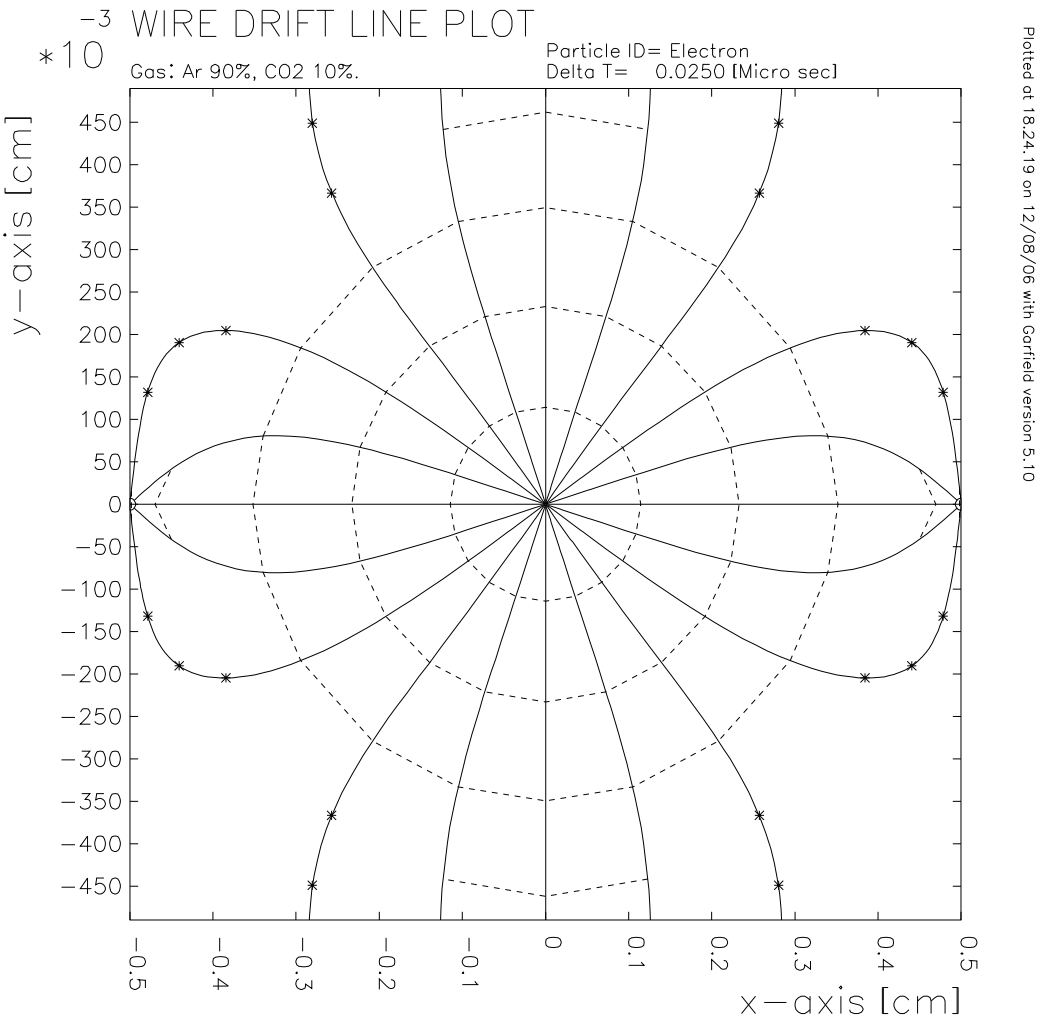

Figure 3: Wire drift line plot for V_s=1650 V, V_f=-300 V.

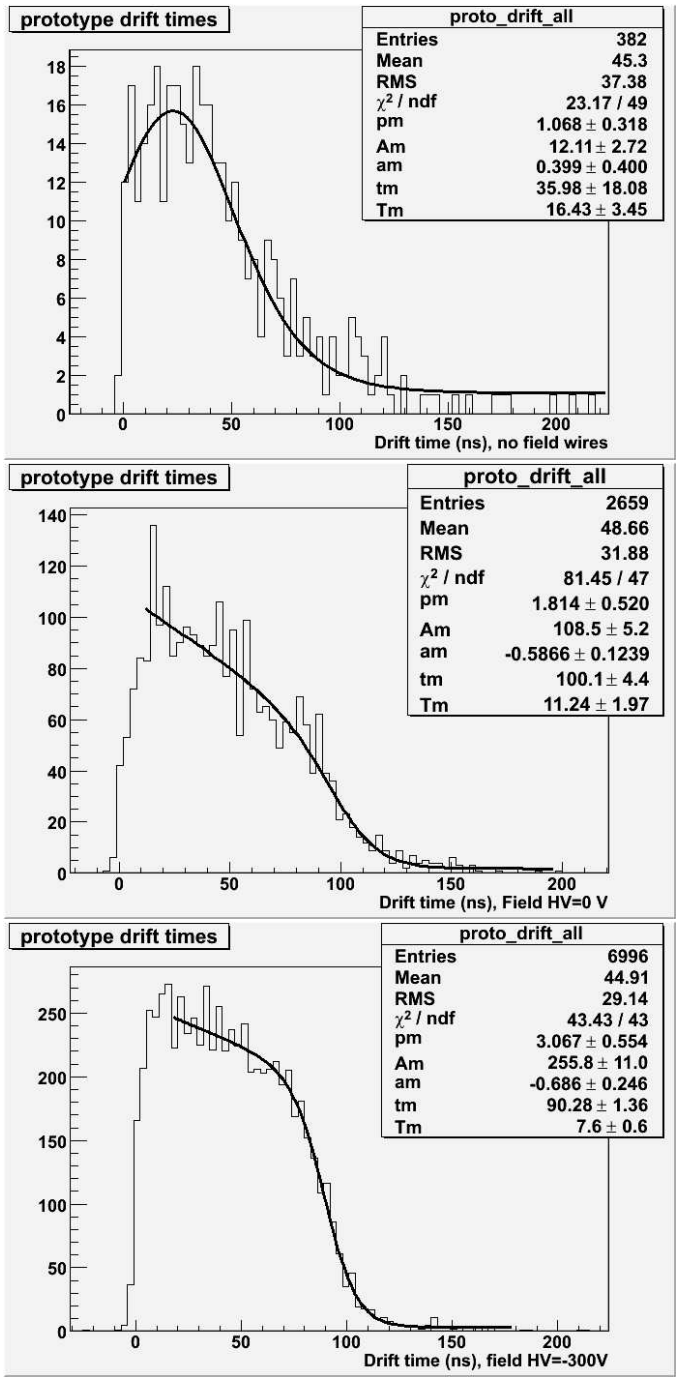

Figure 4: FDC prototype drift distributions for the sense wire only plane with the sense wires at +1750 V (top), the field+sense wire plane with the field wires at zero potential and the sense wires at +1650 V, (middle), and the field+sense wire plane with the field wires at -300 V and the sense wires at +1650 V (bottom).

The readout of the full set of FDC detectors will require on the order of 2850 anode (sense wire) channels and 11400 cathode channels. The exact numbers are subject to the details of the mechanical design, which is presently underway. The signals will be amplified near the detector using an ASIC chip design based on chips used in the ATLAS detector. The nominal data acquisition plan calls for the cathode strips to be read out with 100 MHz Flash-ADCs and the anode wires to be read out with F1 TDCs. We are considering an alternate design in which we would use Flash-ADCs to read out the anode wires as well as the cathode strips.

2 Maintaining the anode-cathode separation

The gain of the FDC chambers depends critically on the gap between the each cathode plane and the anode wires (the "half-gap"). Early cathode plane samples suffered from noticeable folds and wrinkles that lead to local variations in the "half-gap" and hence the gain. Furthermore, little attention was paid to tensioning the cathode planes before they are attached to their frames. When high voltage is applied to the wires, the cathode planes are deflected toward the wires dues to electrostatic pressure as described in [2]. Kapton by itself offers little resistance to this deflection. Our current preferred solution is to attach the Kapton planes to backing material made out of Rohacell®, a very low density foam (ρ=0.032 g/cm^3). A sketch of the various components of a single layer of a package is shown in figure 5.

The presence of the foam increases the multiple scattering in the FDC packages. The foam can in principle be eliminated provided that the cathode planes are appropriately tensioned to minimize deflections. Brian Kross of the Detector Group designed a tensioning mechanism based on two concentric rings. A side view of the apparatus is illustrated in figure 6. The cathode plane ("film" in the diagram) is epoxied face down to the top plate and pulled over the ridge in the bottom plate by using a set of screws at various places around the circumference of the top plate.

The tensioned planes were installed in the small-scale prototype.

The effect of decreasing the half-gap on cathode signals was studied by the ATLAS group for a cathode strip chamber similar to our prototype. Figure 7 shows the relative change of the cathode signals as a function of the change in the half-gap. Assuming these results can be generalized to our geometry, we have set a flatness goal of ± 50 μm, corresponding to a change in the

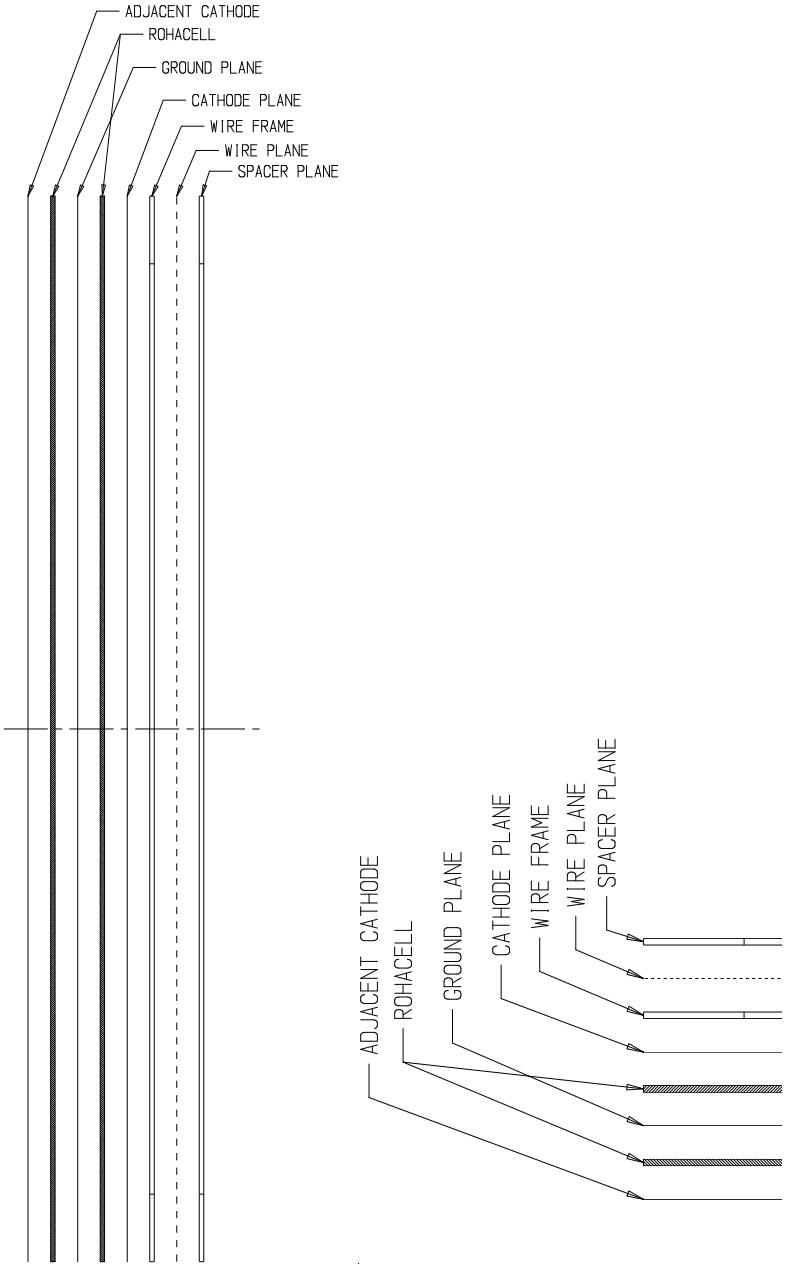

Figure 5: Sketch of the proposed structural components for one cathode-anode-cathode layer of the FDC. The structure repeats 6 times per package.

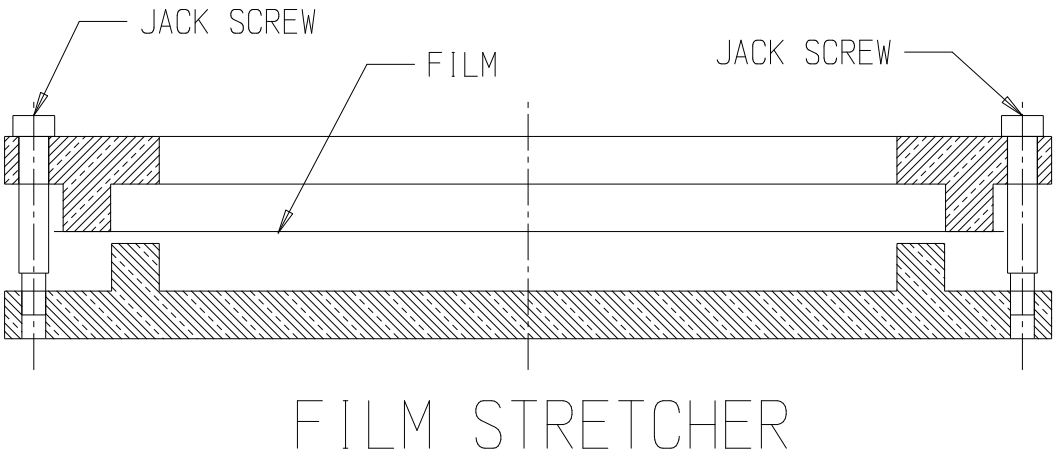

Figure 6: Side view of apparatus for tensioning the cathode planes.

cathode signals of $\pm 5\%$.

3 Field+sense wire results

This report presents the first results for the field+sense wire configuration of the anode plane. Figure 8 shows the efficiency as a function of the voltage applied to the sense wires, with the field wires at zero potential. The efficiency is defined to be the ratio of the number of events that have one peak in each cathode view matched to a sense wire relative to the number of triggers. A narrow plateau occurs above about 1600 V. The setting we used for normal operation was 1650 V. Figure 9 shows the anode charge (deduced from the cathode strip data) as a function of the sense wire high voltage. The trend is well-characterized by Sauli's gain function (equation 31 in [3]). Figure 10 demonstrates that that the position resolution improves with increasing sense wire voltage (and hence gain). It is not feasible to run the chamber with the sense wires at 1700 V because the wires start drawing too much current. However, with the sense wires set at 1650 V, the good resolution obtained

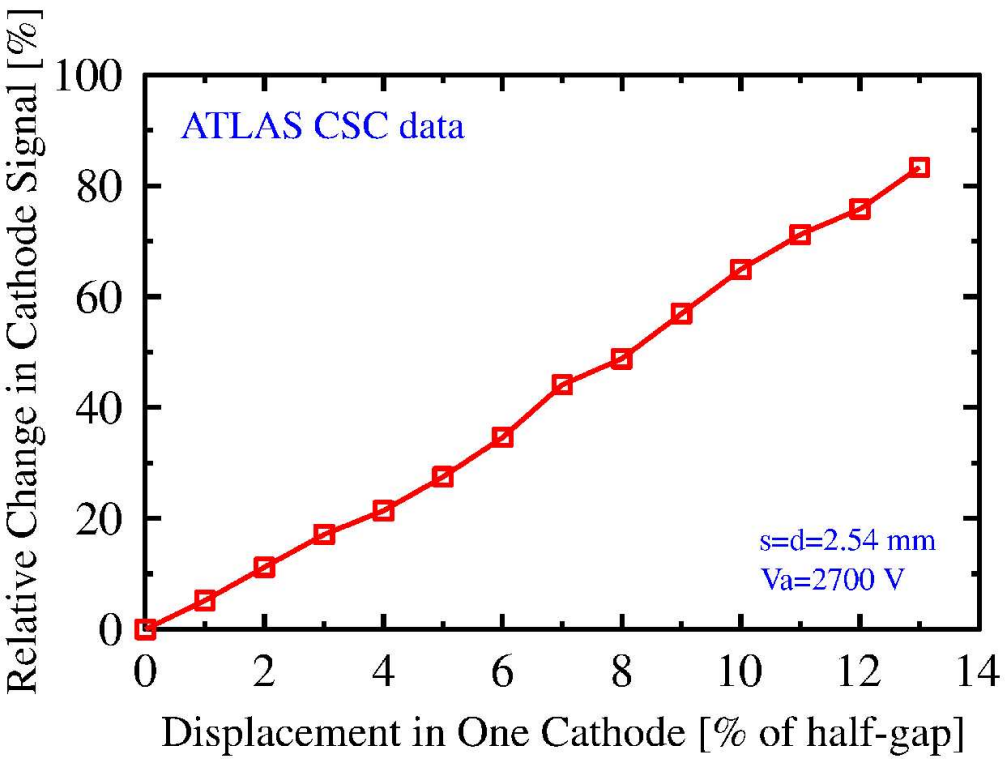

Figure 7: Cathode signal dependence on half-gap from ATLAS CSC data.

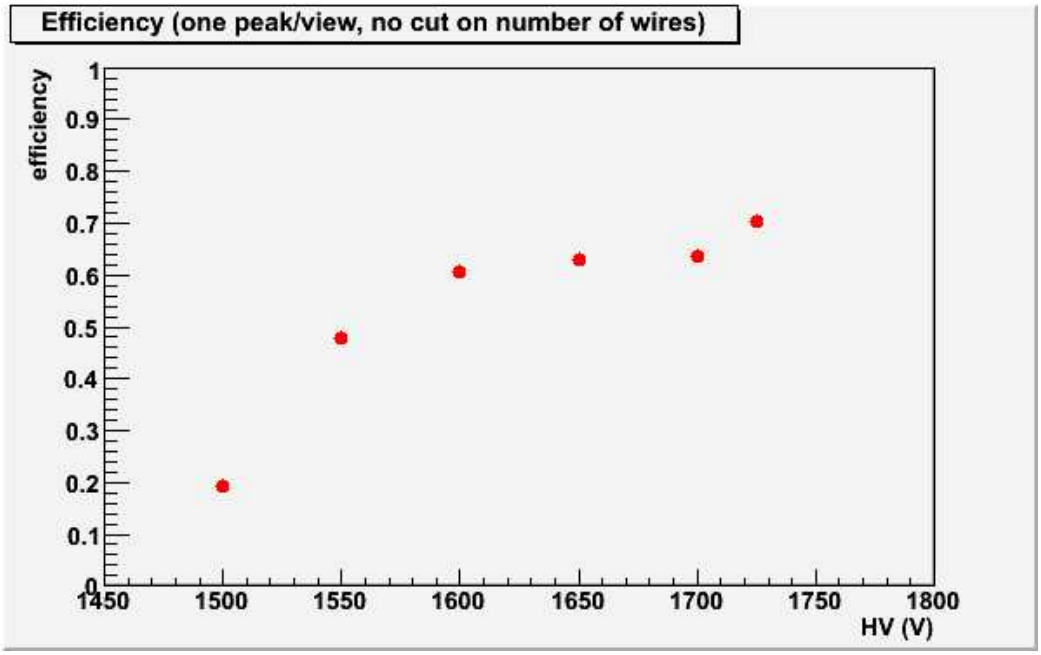

Figure 8: Efficiency as a function of sense wire high voltage for the field+sense wire configuration of the small prototype.

at 1700 V can be recovered by increasing the magnitude of the voltage on the field wires, as demonstrated in figure 11. A plot of the wire positions reconstructed from the cathode data when the sense wires are at +1650 V and the field wires are at -300 V is shown in figure 12. The resolution as a function of x and y is shown in figure 13. The average position resolution under these conditions was 158.2 ± 3.1 μm. This improves upon the typical resolution of 182.6 μm obtained with the sense wire only configuration[4].

The purpose of the cathode tensioning exercise was to make the planes as flat as possible and to minimize electrostatic deflections, thereby minimizing local variations in the gain that could in principle affect the resolution of the device. These "new" planes replaced "old" (untensioned) planes that suffered from numerous folds and wrinkles. Comparisons between the position resolutions obtained for the two configurations as a function of sense high voltage (figure 14) and field high voltage (figure 15) revealed no significant difference between the two sets of planes.

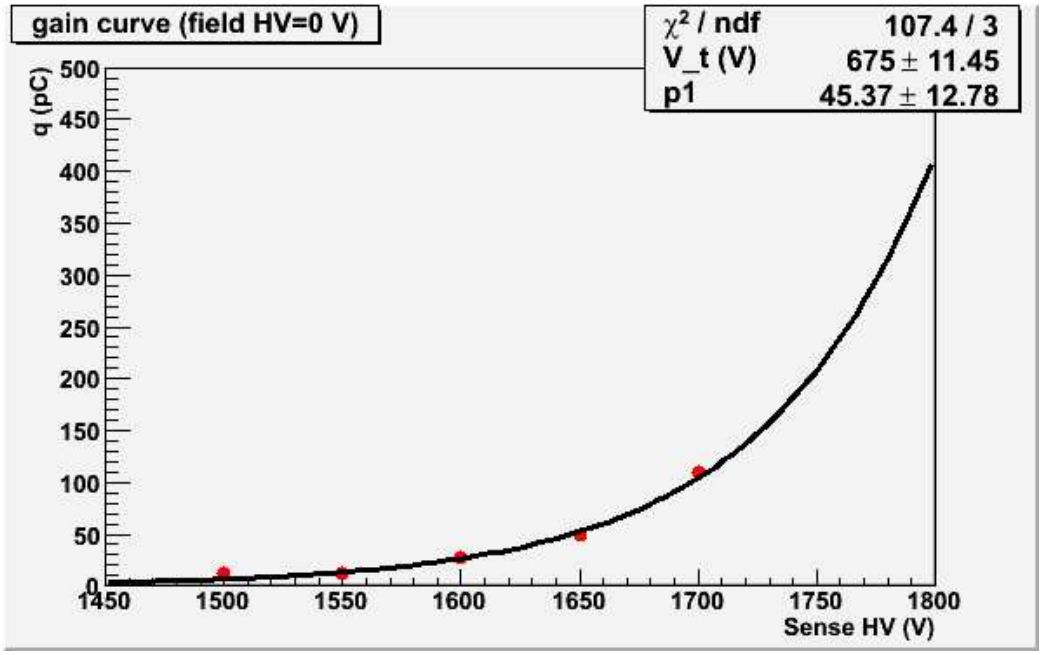

Figure 9: Chamber gain as a function of sense wire voltage with the field wires at zero potential.

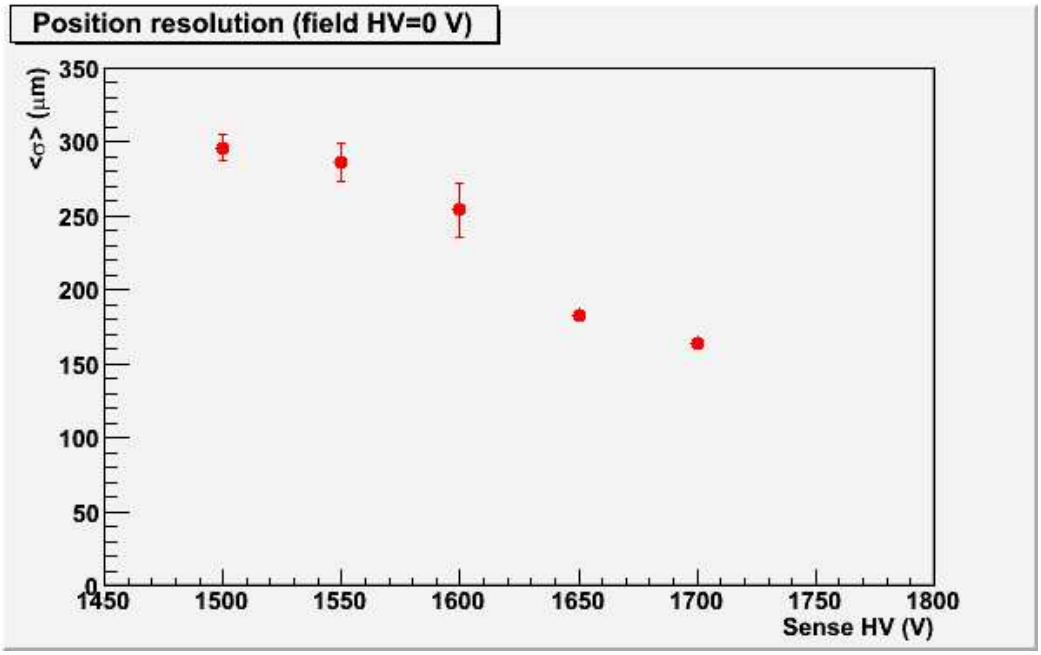

Figure 10: Position resolution as a function of sense wire voltage with the field wires at zero potential.

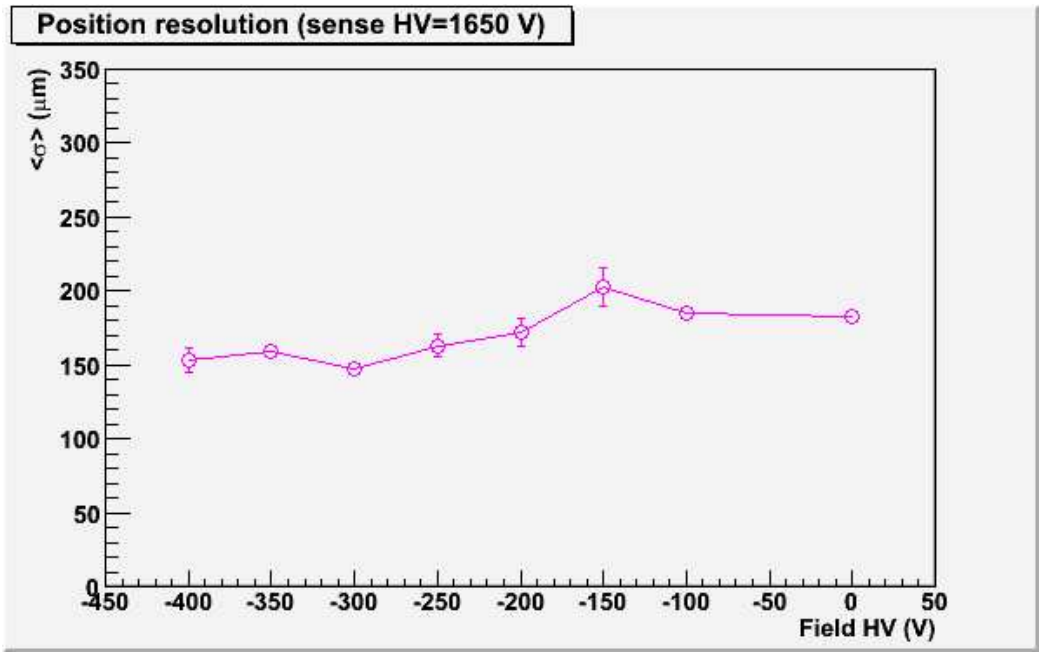

Figure 11: Position resolution as a function of field wire voltage with the sense wires at 1650 V.

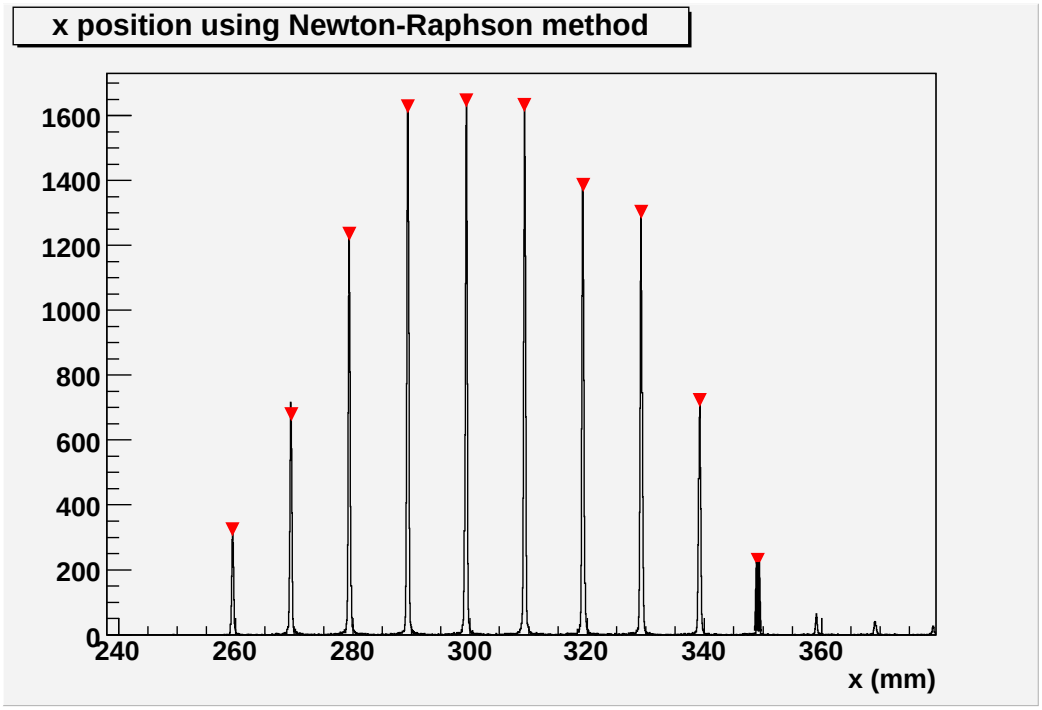

Figure 12: Wire position from cathode data for sense HV=+1650 V, field HV=-300 V

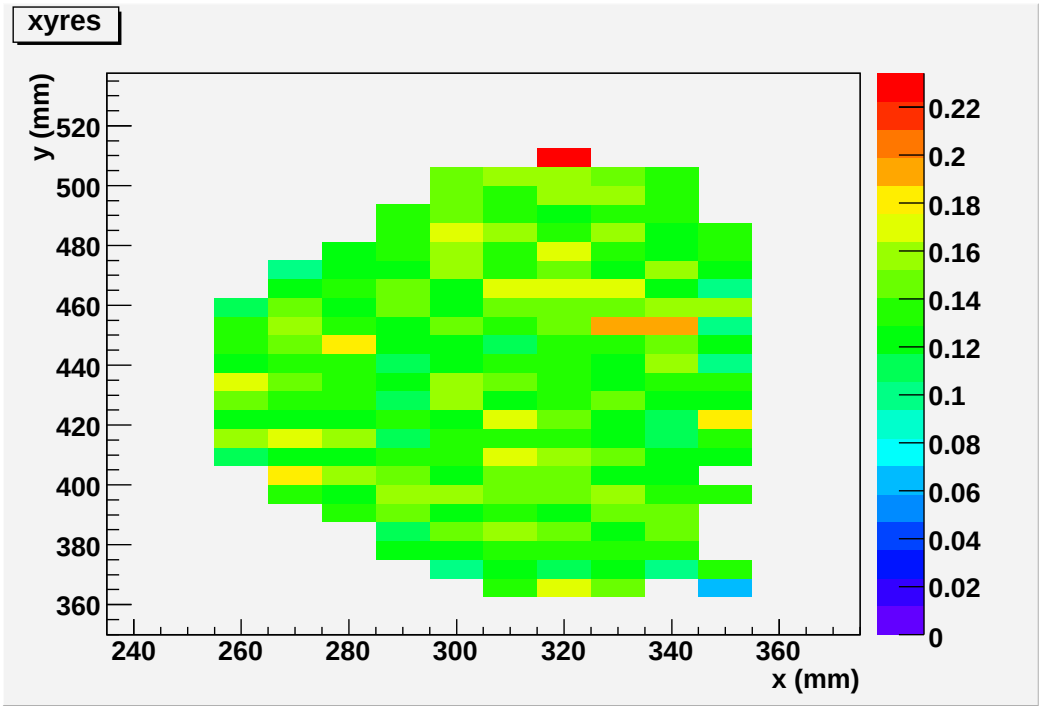

Figure 13: Position resolution as function of position for sense HV=+1650 V, field HV=-300 V

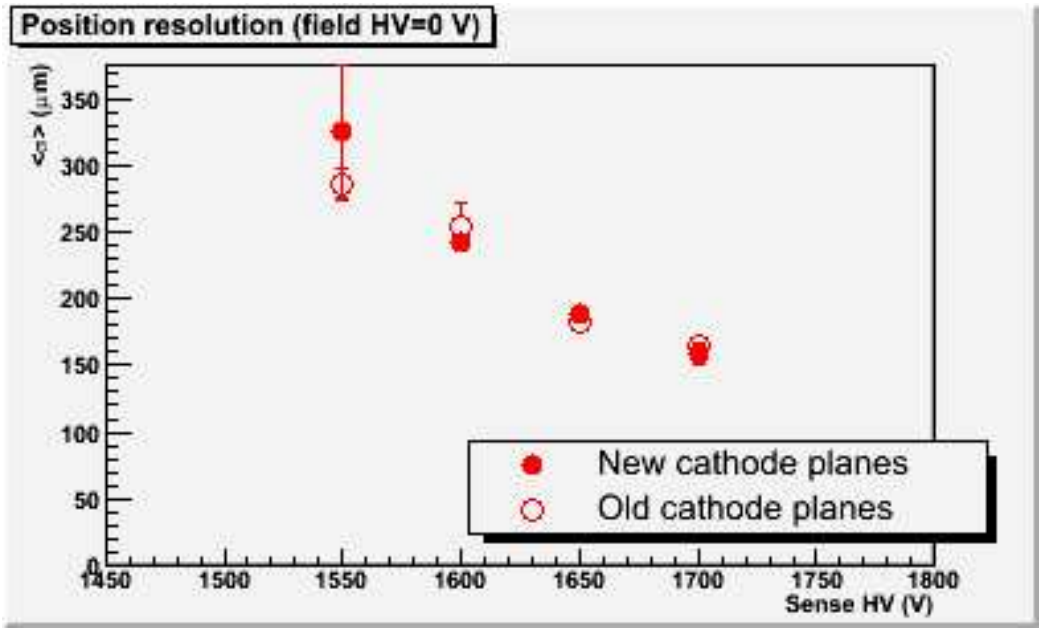

Figure 14: Comparison of position resolution as a function of sense wire high voltage (with the field wires at zero potential) between the "new" (stretched) cathode planes and the "old" (unstretched) cathode planes.

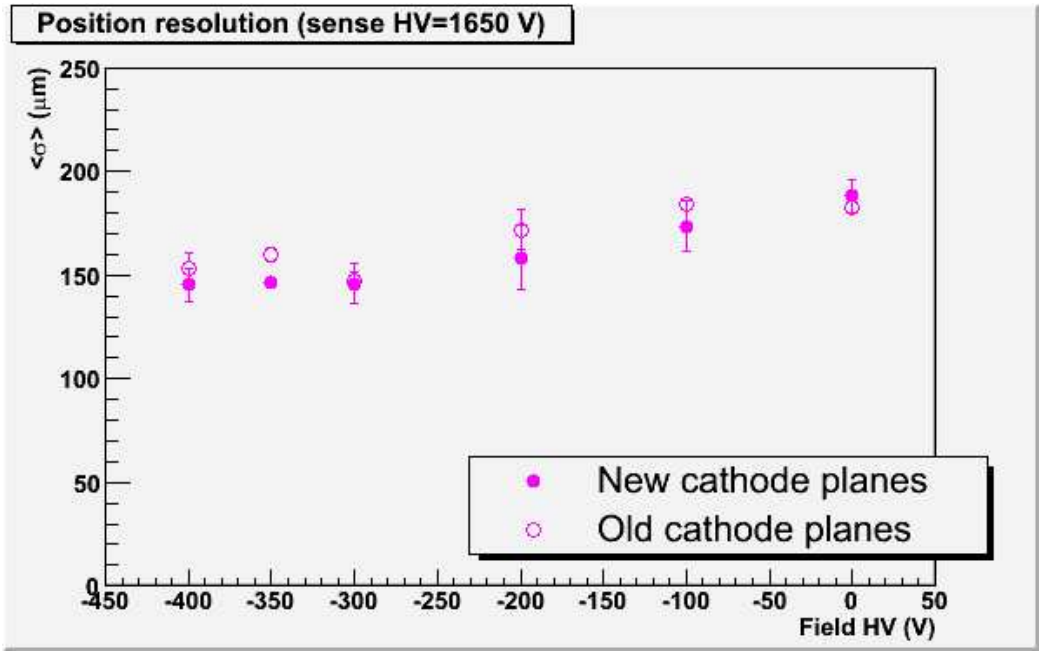

Figure 15: Comparison of position resolution as a function of field wire high voltage (with the sense wires at +1650 V) between the "new" (stretched) cathode planes and the "old" (unstretched) cathode planes.

4 Monte Carlo studies

The active area of the FDC will be limited by the requirement that the frame support the tension on the wires. A study using the Hall-D Geant-based Monte Carlo HDGeant was performed to assess the effect on the acceptance of reducing the active radii of the FDC packages. Single muon tracks were thrown at all angles with respect to the direction of the beam with momenta in the range 0–9 GeV/c. To be accepted the primary track was required to create at least 8 hits in a tracking detector (FDC or CDC). Plots of the detector coverage for several choices of the FDC outer radius are shown in figures 16 and 17. At an outer radius of about 49 cm and below, some events require hits in both the FDC and the CDC to be accepted because there is no longer an overlap between the two detectors. At an outer radius of 33 cm and below, holes in the acceptance start to appear.

References

[1] D. S. Carman, "FDC Garfield Studies v1.0" (http://www.jlab.org/Hall-D/detector/fdc/design/garfield_study.ps).

[2] S. Taylor, GlueX-doc-668-v1.

[3] F. Sauli, "Principles of Operation of Multiwire Proportional and Drift Chambers", CERN 77-09.

[4] S. Taylor and D.S. Carman, GlueX-doc-601-v2.

Legend	
	Kinematical regime covered by CDC only
	Kinematical regime where 8 hits can be obtained from the CDC alone, but the FDC also has some acceptence.
	Kinematical regime where 8 hits can be obtained from either the CDC or the FDC. This is the area where there is the greatest overlap between the CDC and FDC.
	Kinematical regime where 8 hits can be obtained from the FDC alone, but the CDC also has some acceptence.
	Kinematical regime covered by FDC only
	Kinematical regime where hits from **both** the CDC and the FDC are required in order to get at least 8 hits.
	Little or no acceptance

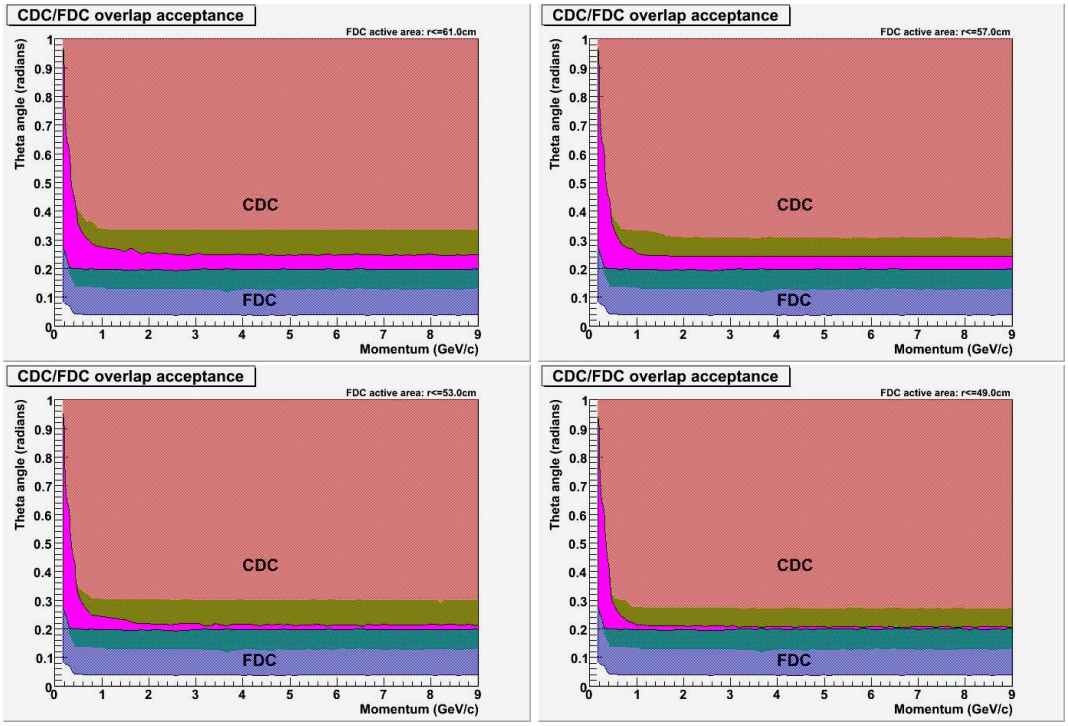

Figure 16: Acceptance as function of momentum and angle for the FDC and CDC. FDC outer radii for left column from top to bottom: r=61 cm, r=53 cm; radii for right column: r=57 cm, r=49 cm.

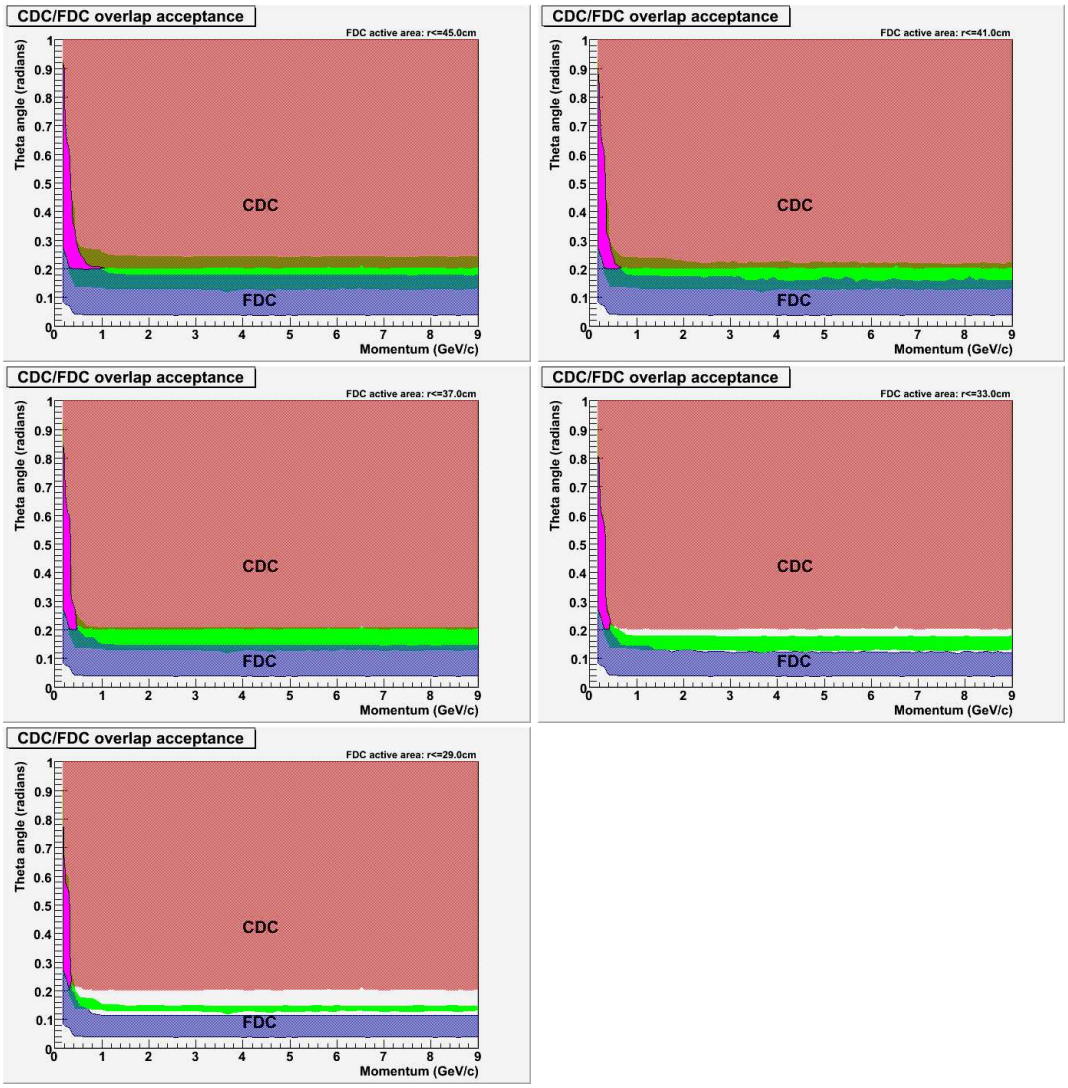

Figure 17: Continuation of figure 16. Left column from top to bottom: r=45 cm, r=37 cm, r=29 cm; right column from top to bottom: r=41 cm, r=33 cm.